Robust Control of Particulate Processes Using Uncertain Population Balances

Timothy Y. Chiu and Panagiotis D. Christofides
Dept. of Chemical Engineering, University of California, Los Angeles, CA 90095

A general method is proposed for the synthesis of robust, nonlinear controllers for spatially homogeneous particulate processes described by population balances including time-varying uncertain variables. The controllers are synthesized via Lyapunov's direct method on the basis of finite-dimensional approximations of the population balances which are obtained by using the method of weighted residuals. The controllers enforce stability in the closed-loop system and attenuation of the effect of uncertain variables on the output, and achieve particle-size distributions with desired characteristics. The robustness of the controllers with respect to unmodeled dynamics is also addressed within the singular perturbation framework. The controllers enforce the desired stability and performance specifications in the closed-loop system, provided that the unmodeled dynamics are stable and sufficiently fast. The proposed control method is applied to a continuous crystallizer with fines trap in which the nucleation rate and the crystal density change arbitrarily with time, and the actuator and sensor dynamics are explicitly considered in the process model, but not included in the model used for controller synthesis. Simulation runs of the closed-loop system clearly demonstrate that the controller attenuates uncertainty, achieves a crystal-size distribution with desired characteristics, and is superior to nonlinear controllers that do not account for the presence of uncertainty.

Introduction

Particulate processes, including crystallizers, emulsion polymerization reactors, and aerosol processes, are widely used in industry for the production of many high-value products including proteins, latex, and powders. The distinct features of particulate processes is the copresence of a continuous phase and a dispersed (particulate) phase, and the occurrence of physicochemical phenomena like particle nucleation, growth, coagulation, and breakage, which are absent in homogeneous processes. The interplay among these phenomena strongly affects the shape of the particle-size distribution (PSD) of the particulate, which in turn determines the physicochemical and mechanical properties of the product made with the particulate. Therefore, it is important to operate particulate processes so that the PSD of the product has a desired shape, even in the presence of significant disturbances.

Fundamental modeling of particulate processes is usually addressed within the framework of population balances, which allow the derivation of systems of nonlinear partial integrodifferential equations that describe the rate of change of the PSD. The population balances are coupled with material and energy balances that describe the rate of change of the state variables of the continuous phase (these are usually systems of nonlinear differential equations that include integrals over the entire particle-size spectrum), leading to complete particulate process models. The complex nature of particulate process models has motivated extensive research efforts on the development of numerical methods for the accurate computation of their solution (see, for example, Landgrebe and Pratsinis, 1990; Hounslow, 1990; Kumar and Ramkrishna, 1996a,b; Hill and Ng, 1996; and the review paper by Ramkrishna, 1985). Furthermore, the strong coupling of the particle nucleation, growth, coagulation, and breakage phenomena and the experimental observations of multiple steady states and sustained oscillations in crystallizers and emulsion polymerization reactors (see the classic book by Randolph and Larson, 1988, for results and references) has motivated many studies on the dynamics of particulate processes (such as Jerauld et al., 1983; Rawlings and Ray, 1987a,b).

Correspondence concerning this article should be addressed to P. D. Christofides.

The highly nonlinear and oscillatory behavior of many particulate processes, together with the need to control the shape of PSDs and the availability of measurement technology that allows the accurate and fast on-line measurement of PSDs, motivates the synthesis and implementation of feedback control systems on particulate processes. In this direction, there is a significant amount of literature (see, for example, Semino and Ray, 1995a, Rohani and Bourne, 1990; Dimitratos et al., 1994, and the references therein) focusing on the use of conventional control schemes (such as proportional-integral and proportional-integral-derivative control, self-tuning control) for the stabilization of crystallizers and emulsion polymerization reactors. Unfortunately, even though these controllers can suppress oscillatory behavior, they cannot effectively control entire size distributions. Therefore, the subject of population balance model-based control of particle-size distribution has received considerable attention over the last 10 years. In this area, important results include optimization-based control (Eaton and Rawlings, 1990), and nonlinear state-feedback control (Kurtz et al., 1998). In Chiu and Christofides (1999), a general model-reduction procedure based on a combination of the method of weighted residuals and approximate inertial manifolds was developed that allows deriving low-order ordinary differential equation (ODE) approximations of particulate process models, which were used for the synthesis of nonlinear low-order output feedback controllers that can be readily implemented in practice. The controllers were successfully implemented on a continuous crystallizer.

In addition to being highly nonlinear and infinite dimensional, the population balance models of most particulate processes are uncertain. Typical sources of model uncertainty include unknown or partially known *time-varying* process parameters, exogenous disturbances, and unmodeled dynamics. It is well known that the presence of uncertain variables and unmodeled dynamics, if not taken into account in the controller design, may lead to severe deterioration of the nominal closed-loop performance or even to closed-loop instability. Research on robust control of nonlinear distributed chemical processes with uncertainty has mainly focused on transport-reaction processes described by nonlinear partial differential equations (PDEs). In this area, important contributions include the development of Lyapunov-based robust control methods for hyperbolic (Christofides and Daoutidis, 1998) and parabolic PDEs (Ydstie and Krishnan, 1994; Ydstie and Alonso, 1997; Christofides, 1998); the reader may refer to the book by Christofides (2000) for detailed results and references in this area. An alternative approach for the design of controllers for PDE systems with *time-invariant* uncertain variables involves the use of adaptive control methods (such as Byrnes, 1987; Wen and Balas, 1989; Demetriou, 1994; Balas, 1995). Despite this progress, at this stage, there is no general framework for the synthesis of practically implementable nonlinear feedback controllers for particulate processes that allow attaining desired particle-size distributions in the presence of significant model uncertainty.

This article focuses on robust control of particulate processes described by uncertain population balances. The objective is to develop a general method for the synthesis of practically implementable robust nonlinear controllers that explicitly handle time-varying uncertain variables (such as unknown process parameters and disturbances) and unmodeled dynamics (such as fast actuator and sensor dynamics not included in the process model). The robust nonlinear controllers enforce stability in the closed-loop system and attenuation of the effect of uncertain variables on the outputs, and achieve particle-size distributions with desired characteristics (such as PSDs with desired total mass, mean particle size).

The article is structured as follows. After introducing the class of particulate process models considered in this work, the method of weighted residuals is used for the construction of finite-dimensional systems that accurately reproduce the dominant dynamics of the particulate process. These ODE systems are subsequently used for the synthesis, via Lyapunov's direct method, of robust nonlinear controllers that enforce stability in the closed-loop system, attenuation of the effect of uncertain variables, and achieve particle-size distributions with desired characteristics. The problem of robustness with respect to unmodeled dynamics is addressed within the singular perturbation framework. It is established that the proposed robust controllers enforce the desired stability and performance specifications in the closed-loop system, provided that the unmodeled dynamics are stable and sufficiently fast. Finally, the proposed robust nonlinear control method is applied to a continuous crystallizer with fines trap, in which the nucleation rate and the crystal density change with time and the actuator and sensor dynamics are explicitly considered in the process model, but not included in the model used for the synthesis of the controller.

Preliminaries

Particulate process model with uncertainty

The mathematical models of particulate processes are typically obtained from an application of a population balance to the particle phase, which accounts for particle growth, nucleation, agglomeration, and breakage, as well as from the application of material and energy balances to the continuous phase. Uncertainty in particulate process models arises from two sources: uncertain variables (such as unknown process parameters and external disturbances) and unmodeled dynamics (such as fast actuator and sensor dynamics, which are not taken into account in the process model). In order to develop a general control method for particulate processes with uncertain variables and unmodeled dynamics, we consider the following singularly perturbed system of nonlinear partial integrodifferential equations

$$\begin{aligned}
\frac{\partial n}{\partial t} &= -\frac{\partial (G(x,r)n)}{\partial r} + \bar{w}[n, x, r, z, \theta(t)] \\
&\quad + \bar{g}_1(n, x, r)u(t), \qquad n(0,t) = b[x(t)] \\
\dot{x} &= \tilde{f}(x) + Q_1(x)z + \bar{g}_2(x)u(t) \\
&\quad + \bar{g}_3\left[x, \theta(t), \int_0^{r_{\max}} a_2(n, r, x)\, dr\right] \\
\epsilon \dot{z} &= \tilde{f}(x) + Q_2(x)z + \tilde{g}_2(x)u(t) \\
&\quad + \tilde{g}_3\left[x, \theta(t), \int_0^{r_{\max}} a_2(n, r, x)\, dr\right], \quad (1)
\end{aligned}$$

where $n(r,t) \in [L_2[0, r_{\max}), \mathbb{R}]$ is the size distribution function that is assumed to be a continuous function of its arguments {we use the symbol $L_2[0, r_{\max})$ to denote a Hilbert space of continuous functions defined on the interval $[0, r_{\max})$}; $r \in [0, r_{\max})$ is the particle size ($r_{\max}$ is the maximum particle size, which may be infinity); t is the time; $x \in \mathbb{R}^n$ is the vector of state variables that describe properties of the continuous phase (such as solute concentration, temperature, and pH in a crystallizer); $u(t) = [u_1 \ u_2 \ \cdots \ u_m]^T \in \mathbb{R}^m$ is the vector of manipulated inputs; $\theta(t) = [\theta_1 \ \theta_2 \ \cdots \ \theta_q]^T \in \mathbb{R}^q$ denotes the vector of uncertain variables; $z \in \mathbb{R}^p$ is the vector of the fast (unmodeled) process dynamics; and ϵ is a small positive parameter that quantifies the speed ratio of the slow vs. the fast dynamical phenomena of the process. $(G, \bar{w}, b)$, $(\bar{g}_1, \bar{f}, \bar{g}_3, \tilde{f}, \tilde{g}_3, a_2)$, and $(Q_1, \bar{g}_2, Q_2, \tilde{g}_2)$ are nonlinear smooth scalar functions, vectors, and matrices, respectively.

In Eq. 1, the n-equation is the population balance where $G(x, r)$ is the growth rate and accounts for particle growth through condensation, and $w[n, x, r, z, \theta(t)]$ is a term that accounts for the net rate of introduction of new particles into the system (it includes all the means by which particles appear or disappear within the system, including particle agglomeration, breakage, nucleation, feed, and removal). The x-subsystem of Eq. 1 is derived by applying material and energy balances to the continuous phase, while the z-subsystem of Eq. 1 represents the fast dynamics that are present in the process but are neglected in the model used for controller design. Finally, the terms $\bar{g}_3[x, \theta(t), \int_0^{r_{\max}} a_2(n, r, x)\, dr]$ and $\tilde{g}_3[x, \theta(t), \int_0^{r_{\max}} a_2(n, r, x)\, dr]$ account for mass and heat transfer from the continuous phase to all the particles in the population.

We define a vector of controlled outputs to express the various control objectives (such as regulation of total number of particles, mean particle size, temperature, pH, etc.) as

$$y_i(t) = h_i\left[\int_0^{r_{\max}} c_\kappa(r)\, n(r,t)\, dr, x\right], \qquad i = 1, \ldots, m, \quad \kappa = 1, \ldots, l, \quad (2)$$

where $y_i(t)$ is the ith controlled output,

$$h_i\left[\int_0^{r_{max}} c_\kappa(r)\, n(r,t)\, dr, x\right]$$

is a nonlinear scalar smooth function of its arguments and $c_\kappa(r)$ is a known smooth function of r that depends on the desired performance specifications.

Throughout the article, we will use the inner product and norm in $L_2[0, r_{\max})$, which are defined, respectively, as

$$(\phi_1, \phi_2) = \int_0^{r_{\max}} \phi_1(z)\, \phi_2(z)\, dz, \quad \|\phi_1\|_2 = (\phi_1, \phi_1)^{1/2}, \quad (3)$$

where ϕ_1, ϕ_2 are two elements of $L_2[0, r_{\max})$. Furthermore, the order of magnitude and Lie derivative notations will be needed in our development. In particular, $\delta(\epsilon) = O(\epsilon)$ if there exist positive real numbers $\bar{k}_1$ and $\bar{k}_2$ such that $|\delta(\epsilon)| \le \bar{k}_1 |\epsilon|$, $\forall |\epsilon| < \bar{k}_2$; $L_f \bar{h}$ denotes the standard Lie derivative of a scalar function $\bar{h}(x)$ with respect to the vector function $f(x)$; $L_f^k \bar{h}$ denotes the kth-order Lie derivative; and $L_g L_f^{k-1} \bar{h}$ denotes the mixed Lie derivative, where $g(x)$ is a vector function.

Remark 1. Referring to the general mathematical model of Eq. 1, the following remarks are in order: (1) the particle-size distribution function $n(r,t)$, is assumed to be a sufficiently smooth function of its arguments [that is, $n(r,t)$ and its partial derivatives with respect to r and t, up to a desired order, are continuous functions]; this is a reasonable assumption for large-size distributions, even though particles are discrete and their number is integer-valued; (2) a single internal particle coordinate (particle size) is considered; this is motivated by the majority of industrial particulate process control problems where the central objective is to produce particulates with a desired particle-size distribution; (3) the particles are assumed to be small enough so that the environment, in which they are dispersed, can be adequately described by a local value of its state vector; (4) we do not consider measured outputs separately from controlled outputs, and thus, we assume that measurements of the $y_i(t)$ are available; and (5) the vector of uncertain variables, $\theta(t)$, and the vector of manipulated inputs, $u(t)$, appear in all the equations of the model.

Remark 2. The derivation of a singularly perturbed representation of a nonlinear process that exhibits two-time-scale behavior is, in general, a highly nontrivial task. The natural approach to address this problem involves defining the singular perturbation parameter, ϵ, taking into account the physicochemical characteristics of the process, so that in the resulting singularly perturbed representation the separation of the fast and slow variables is consistent with the process dynamic behavior. This approach works for the majority of two-time-scale processes (see, for example, the applications considered in Kokotovic et al. (1986). Whenever this approach does not work, alternative approaches that utilize explicit coordinate changes (such as Kokotovic et al., 1986; Kumar et al., 1998) can be employed to derive a singularly perturbed representation of a two-time-scale process. Referring to the specific singularly perturbed system of Eq. 1, we note that the parameter ϵ appears only in the lefthand side (multiplying the time derivative $\dot{z}$), while the fast variable z enters in an affine fashion. The first assumption is made for notational simplicity and can be readily relaxed, while the second assumption is consistent with the fact that in many physical and chemical processes the main nonlinearities are associated with the slow dynamics.

Two-time-scale analysis

The central idea of the two-time-scale analysis is to infer the stability properties of and synthesize well-conditioned nonlinear controllers for the singularly perturbed system of Eq. 1 based on ϵ-independent models that describe the slow and fast dynamics of this system in the slow and fast time-scale, respectively. Setting $\epsilon = 0$ in the system of Eq. 1 and assuming that $Q_2(x, \theta)$ is invertible uniformly in $x \in \mathbb{R}^n$, $\theta \in \mathbb{R}^q$, the following system, which describes the slow dynamics

of the system of Eq. 1 (called slow subsystem), is obtained

$$\frac{\partial n}{\partial t} = -\frac{\partial[G(x,r)n]}{\partial r} + w[n,x,r,\theta(t)] + g_1(n,x,r)u(t), \qquad n(0,t) = b[x(t)]$$
$$\dot{x} = f(x) + g_2(x)u(t) + g_3\left[x, \theta(t), \int_0^{r_{\max}} a_2(n,r,x)\,dr\right], \tag{4}$$

where f, a_2, g_1, g_3, g_2 are nonlinear functions whose explicit form is omitted for brevity. The system that describes the fast dynamics of the system of Eq. 1 (called fast subsystem) can be obtained by defining the fast time-scale $\tau = t/\epsilon$, deriving the representation of the system of Eq. 1 in the τ time scale and setting $\epsilon = 0$, and is of the form

$$\frac{dz}{d\tau} = \tilde{f}(x) + Q_2(x)z + \tilde{g}_2(x)u(t) + \tilde{g}_3\left[x, \theta(t), \int_0^{r_{\max}} a_2(n,r,x)\,dr\right], \tag{5}$$

where x and n can be considered equal to their initial values $x(0)$ and $n(r,0)$, and θ can be viewed as constants. To simplify the development of the theoretical results of the article, we consider systems of the form of Eq. 1, for which the corresponding fast subsystem of the form of Eq. 5 is globally asymptotically stable [that is, the eigenvalues of the matrix $Q_2(x)$ lie in the left half of the complex plane uniformly in $x \in \mathbb{R}^n$].

Remark 3. Whenever the open-loop fast subsystem of Eq. 1 is unstable [that is, one of the eigenvalues of the matrix $Q_2(x)$ lies in the right half of the complex plane] and the pair $[Q_2\ \tilde{g}_2]$ is stabilizable, a preliminary state-feedback law of the form

$$u = k^T(x)z + \tilde{u}, \tag{6}$$

where $\tilde{u}$ is an auxiliary input, can be used to stabilize the fast dynamics, thereby yielding a two-time-scale system with stable fast dynamics. The design of the gain $k^T(x)$ can be performed by using standard optimal control methods (Kokotovic et al., 1986).

Robust Nonlinear Control of Particulate Processes

The objective of this section is to synthesize robust nonlinear controllers for particulate processes of the form of Eq. 4 that enforce stability and robust output tracking in the closed-loop system. Owing to the fact that the unmodeled dynamics in the model of Eq. 1 are stable, the controllers will be synthesized on the basis of the model of Eq. 4. Since this model is infinite-dimensional, we will initially use the method of weighted residuals to derive an ODE approximation of the system of Eq. 4 that will be used for the synthesis of the robust nonlinear controllers.

Model reduction

We initially use the method of weighted residuals to derive a nonlinear set of ODEs that accurately reproduces the solutions and the dominant dynamics of the distributed parameter system of Eq. 4. The central idea of the method of weighted residuals is to approximate the exact solution of $n(r,t)$ by an infinite series of orthogonal basis functions defined in the interval $[0, r_{\max})$ with time-varying coefficients, substitute the series expansion into Eq. 4, and then take the inner product with respect to a complete set of weighted functions, to compute a set of ODEs that describes the rate of change of the time-varying coefficients of the series expansion of the solution. Specifically, we expand the solution of $n(r,t)$ in an infinite series in terms of an orthogonal and complete set of basis functions, $\phi_k(r)$, where $r \in [0, r_{\max})$, $k = 1, \ldots, \infty$, as follows

$$n(r,t) = \sum_{k=1}^{\infty} a_k(t)\phi_k(r), \tag{7}$$

where $a_k(t)$ are time-varying coefficients. Substituting the preceding expansion into the particulate process model of Eq. 4, we obtain

$$\sum_{k=1}^{\infty} \phi_k(r)\frac{\partial a_k(t)}{\partial t} = -\sum_{k=1}^{\infty} a_k(t)\frac{\partial[G(x,r)\phi_k(r)]}{\partial r} + w\left[\sum_{k=1}^{\infty} a_k(t)\phi_k(r), x, r, \theta(t)\right] + g_1\left[\sum_{k=1}^{\infty} a_k(t)\phi_k(r), x, r\right]u(t)$$
$$\dot{x} = f(x) + g_2(x)u(t) + g_3\left\{x, \theta(t), \int_0^{r_{\max}} a_2\left[\sum_{k=1}^{\infty} a_k(t)\phi_k(r), r, x\right]dr\right\}. \tag{8}$$

Multiplying the population balance with the weighting functions, $\psi_\nu(r)$, and integrating over the entire particle-size spectrum (that is, taking inner product in $L_2[0, r_{\max})$ with the weighting functions), the following set of infinite ODEs is obtained

$$\int_0^{r_{\max}} \psi_\nu(r)\sum_{k=1}^{\infty} \phi_k(r)\frac{\partial a_k(t)}{\partial t}\,dr = -\sum_{k=1}^{\infty} a_k(t)\int_0^{r_{\max}} \psi_\nu(r)\frac{\partial(G(x,r)\phi_k(r))}{\partial r}\,dr + \int_0^{r_{\max}} \psi_\nu(r) w\left[\sum_{k=1}^{\infty} a_k(t)\phi_k(r), x, r, \theta(t)\right]dr + \int_0^{r_{\max}} \psi_\nu(r) g_1\left[\sum_{k=1}^{\infty} a_k(t)\phi_k(r), x, r\right]u(t)\,dr, \quad \nu = 1, \ldots, \infty$$
$$\dot{x} = f(x) + g_2(x)u(t) + g_3\left\{x, \theta(t), \int_0^{r_{\max}} a_2\left[\sum_{k=1}^{\infty} a_k(t)\phi_k(r), r, x\right]dr\right\}. \tag{9}$$

Equation 9 is an infinite set of ODEs that describe the rate of change of the time-varying coefficients, $a_k(t)$, where $k = 1, \ldots, \infty$, of the series expansion of the solution. An accurate approximation of Eq. 9 is obtained by truncating the series expansion of $n(r,t)$ up to order N and taking the first N

equations (that is, $\nu = 1, \ldots, N$). The infinite-dimensional system of Eq. 9 reduces to the following finite set of ODEs

$$\begin{aligned}
&\int_0^{r_{\max}} \psi_\nu(r) \sum_{k=1}^{N} \phi_k(r) \frac{\partial a_{kN}(t)}{\partial t}\, dr \\
&\quad = -\sum_{k=1}^{N} a_{KN}(t) \int_0^{r_{\max}} \psi_\nu(r) \frac{\partial \left[G(x_N, r)\phi_k(r) \right]}{\partial r}\, dr \\
&\quad + \int_0^{r_{\max}} \psi_\nu(r) w\left[\sum_{k=1}^{N} a_{kN}(t)\phi_k(r), x_N, r, \theta(t) \right] dr \\
&\quad + \int_0^{r_{\max}} \psi_\nu(r) g_1\left[\sum_{k=1}^{N} a_{kN}(t)\phi_k(r), x_N, r \right] u(t)\, dr, \\
&\qquad\qquad\qquad\qquad\qquad\qquad\qquad\qquad \nu = 1, \ldots, N \\
&\dot{x}_N = f(x_N) + g_2(x_N)u(t) \\
&\quad + g_3\left\{ x_N, \theta(t), \int_0^{r_{\max}} a_2\left[\sum_{k=1}^{N} a_{kN}(t)\phi_k(r), r, x_N \right] dr \right\},
\end{aligned} \tag{10}$$

where x_N and a_{kN} are the approximations of x and a_k obtained by an Nth-order truncation. Introducing the vector notation $a_N = [a_{1N} \cdots a_{NN}]$, and after some rearrangements, Eq. 10 can be represented in the following general form

$$\begin{aligned}
\dot{a}_N &= \bar{f}\left[a_N, x_N, \theta(t) \right] + \bar{g}(a_N, x_N)u(t) \\
\dot{x}_N &= f(x_N) + g_2(x_N)u(t) + g_3\left[x_N, a_N, \theta(t) \right],
\end{aligned} \tag{11}$$

where the explicit expressions of $\bar{f}(a_N, x_N, \theta(t))$ and $\bar{g}(a_N, x_N)$ are omitted for brevity. Setting $\tilde{x} = [a_N^T \; x_N^T]^T$, we obtain the following system

$$\begin{aligned}
\dot{\tilde{x}} &= \tilde{f}(\tilde{x}) + \sum_{i=1}^{m} \tilde{g}_i(\tilde{x})u_i + \tilde{w}(\tilde{x}, \theta) \\
y_{s_i} &= \tilde{h}_i(\tilde{x}), \qquad i = 1, \ldots, m,
\end{aligned} \tag{12}$$

where $\tilde{f}(\tilde{x})$, $\tilde{g}_i(\tilde{x})$, $\tilde{w}(\tilde{x}, \theta)$ are nonlinear vector functions whose explicit form is omitted brevity.

Remark 4. In the series expansion of Eq. 7, the basis, $\{\phi_k\}$, $j = 1, \ldots, \infty$, of $L_2[0, r_{\max})$ can be chosen from standard basis functions sets (for example, when $r_{\max} = \infty$, $\{\phi_k\}$ can be chosen to be Laguerre polynomials; see the crystallization example in the fourth section for details on this issue), or it can be computed by applying the Karhunen-Loève expansion on an appropriately chosen ensemble of solutions of the system of Eq. 4 [see Holmes et al. (1996) for details on the Karhunen-Loève expansion].

Remark 5. The method of weighted residuals reduces to the method of moments when the basis functions are chosen to be Laguerre polynomials and the weighting functions are chosen as $\psi_\nu = r^\nu$. The moments of the particle-size distribution are defined as

$$\mu_\nu = \int_0^\infty r^\nu n(r, t)\, dr, \qquad \nu = 0, \ldots, \infty, \tag{13}$$

and the moment equations can be directly generated from the population balance model by multiplying it by r^ν, $\nu = 0, \ldots, \infty$ and integrating from 0 to ∞. The procedure of forming moments of the population-balance equation very often leads to terms that may not reduce to moments, terms that include fractional moments, or to an unclosed set of moment equations. To overcome this problem, the particle-size distribution is expanded in terms of Laguerre polynomials defined in $L_2[0, \infty)$ and the series solution is used to close the set of moment equations.

Remark 6. When an arbitrary set of basis functions is used in the expansion of Eq. 7, the ODE system of Eq. 11 may be of very high order in order to accurately describe the dominant dynamics of the system of Eq. 4, and therefore, to be suitable for the synthesis of a high-performance nonlinear controller. Unfortunately, high dimensionality of the system of Eq. 11 leads to a complex controller design and high-order controllers, which cannot be readily implemented in practice. An approach to overcome this problem is to reduce the dimension of the system of Eq. 11 utilizing the concept of approximate inertial manifold for particulate process models proposed in Chiu and Christofides (1999).

Robust nonlinear controller design

The objective of this subsection is to use the ODE system of Eq. 12 to synthesize robust state-feedback controllers of the form

$$u = p(\tilde{x}) + Q(\tilde{x})\bar{v} + r(\tilde{x}, t), \tag{14}$$

where $p(\tilde{x})$, $r(\tilde{x}, t)$ are vector functions; $Q(\tilde{x})$ is a matrix; and $\bar{v}$ is a vector of the form $\bar{v} = \mathbf{v}(v_i, v_i^{(1)}, \ldots, v_i^{(r_i)})$—where $\mathbf{v}(v_i, v_i^{(1)}, \ldots, v_i^{(r_i)})$ is a smooth vector function, $v_i^{(k)}$ is the kth time derivative of the external reference input v_i (which is assumed to be a smooth function of time), and r_i is a positive integer—which enforce boundedness of the states and output tracking with arbitrary degree of asymptotic attenuation of the effect of the uncertainty on the output, in the closed-loop system, provided that ϵ is sufficiently small (that is, the unmodeled dynamics are sufficiently fast). The control law of Eq. 14 comprises the component $p(\tilde{x}) + Q(\tilde{x})\bar{v}$, which is responsible for the output tracking and stabilization of the closed-loop slow system, and the component $r(\tilde{x}, t)$, which is responsible for the asymptotic attenuation of the effect of the uncertain variables on the outputs of the system of Eq. 12. The control law of Eq. 14 will be synthesized constructively using Lyapunov's direct method, and assuming the existence of known bounding functions that capture the magnitude of the uncertain terms and that certain structural conditions on the way the uncertain variables affect the output are satisfied. Finally, the reader can refer to Remark 9 for results on the implementation of a control law of the form of Eq. 14 with a state observer, when measurements of the states of the system of Eq. 1 are not available.

In order to develop a solution to the preceding robust control problem, we will need to impose the following three assumptions on the system of Eq. 12. We initially assume that there exists a coordinate transformation that renders the system of Eq. 12 partially linear. This assumption is motivated by the requirement of robust output tracking and is precisely formulated below:

Assumption 1. Referring to the system of Eq. 12, there exist a set of integers $(r_1, r_2, \ldots, r_m)$ and a coordinate trans-

formation $(\zeta, \eta) = T(x_s, \theta)$ such that the representation of the system, in the coordinates (ζ, η), takes the form

$$\begin{aligned}
\dot{\zeta}_1^{(1)} &= \zeta_2^{(1)} \\
&\vdots \\
\dot{\zeta}_{r_1-1}^{(1)} &= \zeta_{r_1}^{(1)} \\
\dot{\zeta}_{r_1}^{(1)} &= L_{\tilde{f}}^{r_1}\tilde{h}_1(\tilde{x}) + \sum_{i=1}^{m} L_{\tilde{g}_i} L_{\tilde{f}}^{r_1-1}\tilde{h}_1(\tilde{x})u_i + L_{\tilde{w}} L_{\tilde{f}}^{r_1-1}\tilde{h}_1(\tilde{x}) \\
&\vdots \\
\dot{\zeta}_1^{(m)} &= \zeta_2^{(m)} \\
&\vdots \\
\dot{\zeta}_{r_m-1}^{(m)} &= \zeta_{r_m}^{(l)} \\
\dot{\zeta}_{r_m}^{(m)} &= L_{\tilde{f}}^{r_m}\tilde{h}_m(\tilde{x}) + \sum_{i=1}^{m} L_{\tilde{g}_i} L_{\tilde{f}}^{r_m-1}\tilde{h}_m(\tilde{x})u_i \\
&\qquad + L_{\tilde{w}} L_{\tilde{f}}^{r_m-1}\tilde{h}_m(\tilde{x}) \\
\dot{\eta}_1 &= \Psi_1(\zeta, \eta, \theta, \dot{\theta}) \\
&\vdots \\
\dot{\eta}_{(n+N)-\Sigma_i r_i} &= \Psi_{(n+N)-\Sigma_i r_i}(\zeta, \eta, \theta, \dot{\theta}) \\
y_{s_i} &= \zeta_1^{(i)}, \qquad i = 1, \ldots, m,
\end{aligned} \tag{15}$$

where

$$\begin{aligned}
x_s &= T^{-1}(\zeta, \eta, \theta), \\
\zeta &= \left[\zeta^{(1)} \ \ldots \ \zeta^{(m)}\right]^T \in \mathbb{R}^{\Sigma_i r_i}, \\
\eta &= \left[\eta_1 \ \cdots \ \eta_{(n+N)-\Sigma_i r_i}\right]^T \in \mathbb{R}^{(n+N)-\Sigma_i r_i}.
\end{aligned}$$

Assumption 1 includes the matching condition of our robust control methodology. In particular, we consider systems of the form Eq. 12 for which the time-derivatives of the output y_{si} up to order $r_i - 1$ are independent of the vector of uncertain variables θ. Notice that this condition is different from the standard one that restricts the uncertainty vector θ to enter the systems of Eq. 12 in the same equation with the manipulated input u. The motivation for considering this matching condition is given by the fact that it is satisfied by a large number of practical applications (note that Assumption 1 is always satisfied for system for which $r_i = 1$, for all $i = 1, \ldots, m$).

Referring to the system of Eq. 12, we will assume, in order to simplify the presentation of our results, that the matrix

$$C(\tilde{x}) = \begin{bmatrix} L_{\tilde{g}_1} L_{\tilde{f}}^{r_1-1}\tilde{h}_1(\tilde{x}) & \cdots & L_{\tilde{g}_m} L_{\tilde{f}}^{r_1-1}\tilde{h}_1(\tilde{x}) \\ \vdots & \cdots & \vdots \\ L_{\tilde{g}_1} L_{\tilde{f}}^{r_m-1}\tilde{h}_m(\tilde{x}) & \cdots & L_{\tilde{g}_m} L_{\tilde{f}}^{r_m-1}\tilde{h}_m(\tilde{x}) \end{bmatrix} \tag{16}$$

is nonsingular uniformly in $\tilde{x}$. This assumption can be readily relaxed if robust dynamic state feedback, instead of robust state feedback, is used to solve the control problem [see Isidori (1989) for details].

The next assumption is made to ensure bounded stability of the internal dynamics of the system of Eq. 12 under a robust state-feedback controller of the form of Eq. 12.

Assumption 2. The dynamical system

$$\begin{aligned}
\dot{\eta}_1 &= \Psi_1(\zeta, 0, 0, 0) \\
&\vdots \\
\dot{\eta}_{(n+N)-\Sigma_i r_i} &= \Psi_{(n+N)-\Sigma_i r_i}(\zeta, 0, 0, 0)
\end{aligned} \tag{17}$$

is locally exponentially stable.

Finally, we need to assume that there exists a nonlinear time-varying function that captures the size of the uncertain term $[L_{\tilde{w}} L_{\tilde{f}}^{r_1-1}\tilde{h}_1(\tilde{x}) \ \cdots \ L_{\tilde{w}} L_{\tilde{f}}^{r_m-1}\tilde{h}_m(\tilde{x})]$. Information of this kind can result from physical considerations, preliminary simulations, and experimental data (for example, when the pre-exponential constant in the nucleation law is not exactly known, experimental information can be used to obtain the range of variation of this parameter and compute a bound on the preceding uncertain term).

Assumption 3. There exists a known function $c(\tilde{x}, t)$ such that the following condition holds

$$\left|\left[L_{\tilde{w}} L_{\tilde{f}}^{r_1-1}\tilde{h}_1(\tilde{x}) \ \cdots \ L_{\tilde{w}} L_{\tilde{f}}^{r_m-1}\tilde{h}_m(\tilde{x})\right]^T\right| \le c(\tilde{x}, t) \tag{18}$$

for all $\tilde{x} \in \mathbb{R}^{n+N}$, $\theta \in \mathbb{R}^q$, $t \ge 0$.

Theorem 1, which follows, provides an explicit formula for the robust controller, conditions that ensure boundedness of the state, and a precise characterization of the ultimate uncertainty attenuation level. To simplify the statement of the theorem, we set $\bar{v}_i = [v_i \ v_i^{(1)} \ldots v_i^{(r_i)}]^T$ and $\tilde{v} = [\bar{v}_1^T \ \bar{v}_2^T \cdots \bar{v}_m^T]^T$.

Theorem 1. Suppose that Assumptions 1, 2, and 3 hold, and consider the system of Eq. 1 under the robust state feedback controller

$$\begin{aligned}
u &= a(\tilde{x}, \tilde{v}, t) \\
&:= [C(\tilde{x})]^{-1} \left\{ \sum_{i=1}^{m} \sum_{k=1}^{r_i} \frac{\beta_{ik}}{\beta_{ir_i}} \left[v_i^{(k)} - L_{\tilde{f}}^{k}\tilde{h}_i(\tilde{x}) \right] \right. \\
&\quad + \sum_{i=1}^{m} \sum_{k=1}^{r_i} \frac{\beta_{ik}}{\beta_{ir_i}} \left[v_i^{(k-1)} - L_{\tilde{f}}^{k-1}\tilde{h}_i(\tilde{x}) \right] \\
&\quad \left. - \chi[c(\tilde{x}, t)] \frac{\sum_{i=1}^{l} \sum_{k=1}^{r_i} \frac{\beta_{ik}}{\beta_{ir_i}} \left[L_{\tilde{f}}^{k-1}\tilde{h}_i(\tilde{x}) - v_i^{(k-1)} \right]}{\left| \sum_{i=1}^{l} \sum_{k=1}^{r_i} \frac{\beta_{ik}}{\beta_{ir_i}} \left[L_{\tilde{f}}^{k-1}\tilde{h}_i(\tilde{x}) - v_i^{(k-1)} \right] \right| + \phi} \right\},
\end{aligned} \tag{19}$$

where

$$\frac{\beta_{ik}}{\beta_{ir_i}} = \left[\frac{\beta_{ik}^1}{\beta_{ir_i}^1} \cdots \frac{\beta_{ik}^l}{\beta_{ir_i}^l} \right]^T$$

are column vectors of parameters chosen so that the roots of the equation $\det(B(s)) = 0$, where $B(s)$ is an $m \times m$ matrix,

whose (i, j)th element is of the form $\sum_{k=1}^{r_i}(\beta_{jk}^i/\beta_{jr_i}^i)s^{k-1}$, lie in the open left half of the complex plane, and χ, ϕ are adjustable parameters with $\chi > 1$ and $\phi > 0$. Then, there exist positive real numbers (δ, ϕ^*, d) such that for each $\phi \le \phi^*$, there exists $\epsilon^*(\phi)$, such that if $\phi \le \phi^*$, $\epsilon \le \epsilon^*(\phi)$ and $\max\{|x(0)|, |z(0)|, \|n(r,0)\|_2, \|\theta\|, \|\dot{\theta}\|, \|\tilde{v}\|\} \le \delta$:

(a) The state of the infinite-dimensional closed-loop system is bounded.

(b) The outputs of the infinite-dimensional closed-loop system satisfy.

$$\limsup_{t \to \infty} |y_i - v_i| \le d, \qquad i = 1, \ldots, l \tag{20}$$

Remark 7. Regarding the practical application of Theorem 1, one has to initially use the method of weighted residuals to derive an ODE system of the form of Eq. 12, and then verify Assumptions 1, 2, and 3 on the basis of this system. Then, the synthesis formula of Eq. 19 can be directly used to derive the explicit form of the controller. Moreover, the value of ϵ in the model of Eq. 1 is typically fixed by the process, say ϵ_p, and thus there is a limit on how small the ultimate bound d can be chosen. For example, one can initially compute, through simulations, a ϕ^* from the desired (δ, d) and, in turn, the value ϵ^* for $\phi \le \phi^*$. If this ϵ^* is less than ϵ_p, then d may need to be readjusted (increased) so that $\epsilon^* \ge \epsilon_p$. Of course, if ϵ_p is too large, there may be no value of d that works.

Remark 8. Referring to the robust nonlinear controller of Eq. 19, we note that the nonlinear term $-\chi[c(\tilde{x}, t)]$ could have been replaced by a sufficiently large positive constant k. Although this modification would lead to a simplification in the practical implementation of the controller, we elect to use the nonlinear term, because the use of a large positive constant results in a controller that computes very large control action, when the discrepancy between y and v (tracking error) is far from being zero. The controller that uses the nonlinear term avoids this problem and does not compute unnecessarily large control action (see the manipulated input profiles for the crystallizer example presented in the next section).

Remark 9. The on-line implementation of the controller of Eq. 19 requires that the values of the state variables $\tilde{x}$ are known. Unfortunately, $\tilde{x}$ may not be known in many practical applications. One way to address this problem is to use a nonlinear state observer of the form

$$\frac{d\omega}{dt} = \tilde{f}(\omega) + \tilde{g}(\omega)u + \tilde{w}(\omega)\theta_n + L\left[y - \tilde{h}(\omega)\right], \tag{21}$$

where ω denotes the observer state vector (the dimension of the vector ω is equal to the dimension of $\tilde{x}$ in the system of Eq. 12); $y = [y_1\ y_2\ \cdots\ y_m]^T$ is the measured output vector; θ_n denotes a nominal value for $\theta(t)$; and L is an $(n \times m)$ matrix chosen so that the eigenvalues of the matrix

$$C_L = \frac{\partial \tilde{f}}{\partial \omega}_{(\omega = \omega_s)} - L\frac{\partial \tilde{h}}{\partial \omega}_{(\omega = \omega_s)},$$

where ω_s is the operating steady state, $\partial\tilde{f}/\partial\omega$ is an $(n \times n)$ Jacobian matrix, and $\partial\tilde{h}/\partial\omega$ is an $(m \times n)$ Jacobian matrix, lie in the open left-half of the complex plane, to estimate $\tilde{x}$ from measurements of the controlled outputs y_i. The state observer of Eq. 21 consists of a replica of the system of Eq. 12 plus a linear gain multiplying the discrepancy between the actual and the estimated value of the output, and therefore it is an extended Luenberger-type observer. It can be shown [see, for example, Daoutidis and Christofides (1995), Christofides (2000), for techniques to prove such a result] that the local bounded stability of the closed-loop system resulting from the application of a robust output feedback controller (resulting from the combination of the controller of Eq. 19 with the observer of Eq. 21) to the particulate process model is guaranteed, provided that there exists a matrix L such that $C_L = (1/\mu)\bar{A}$, where μ is a sufficiently small positive parameter and $\bar{A}$ is a Hurwitz matrix. The reader may refer to the crystallization example of the next section for an application of this approach for state estimation.

Remark 10. We note that the validity of the approach that we followed here to synthesize the nonlinear robust controller of Eq. 19 relies on the large separation of slow and fast modes of the particulate process model of Eq. 4. Despite the fact that the model of Eq. 22 consists of a first-order hyperbolic PDE (population balance) coupled with a nonlinear integrodifferential equation (solute mass balance), the approach followed here for the synthesis of robust feedback controllers is not applicable to hyperbolic PDE systems arising in the context of convection-reaction processes. More specifically, the dominant dynamic behavior of the system of Eq. 4 is characterized by a small number of degrees of freedom (and thus, it can be described by low-order ODE systems that can be used for controller synthesis), while first-order hyperbolic PDE systems involve spatial differential operators whose eigenvalues cluster along vertical or nearly vertical asymptotes in the complex plane, and thus the controller synthesis problem has to be addressed directly on the basis of the hyperbolic PDE system (see Christofides and Daoutidis, 1998).

Application to a Continuous Crystallizer with Fines Trap

In this section, we apply the proposed robust control methodology to a continuous crystallizer with fines trap shown in Figure 1. The trap is used to remove small crystals and increase the mean crystal size. In a crystallizer, the precise regulation of the shape of the crystal-size distribution (CSD) is important because the CSD influences significantly the necessary liquid–solid separation and the properties of the product. Therefore, crystallization requires a population balance in order to be accurately described, analyzed, and controlled. Under the standard assumptions of constant volume, mixed suspension, mixed product removal, and nucleation of crystals of infinitesimal size, application of a population balance of the particulate phase and a mass balance to the continuous phase results in the following dynamic model for the crystallizer (Lei et al., 1971)

$$\frac{\partial n}{\partial \bar{t}} = -\frac{\partial\left(R(\bar{t})n\right)}{\partial r} - \frac{n}{\tau} - \bar{h}(r)\frac{n}{\tilde{\tau}} + \delta(r-0)Q(\tilde{t})$$

$$\frac{dc}{d\bar{t}} = \frac{(c_0 - \rho)}{\bar{\epsilon}\tau} + \frac{(\rho - c)}{\tau} + \frac{(\rho - c)}{\bar{\epsilon}}\frac{d\bar{\epsilon}}{d\bar{t}}, \tag{22}$$

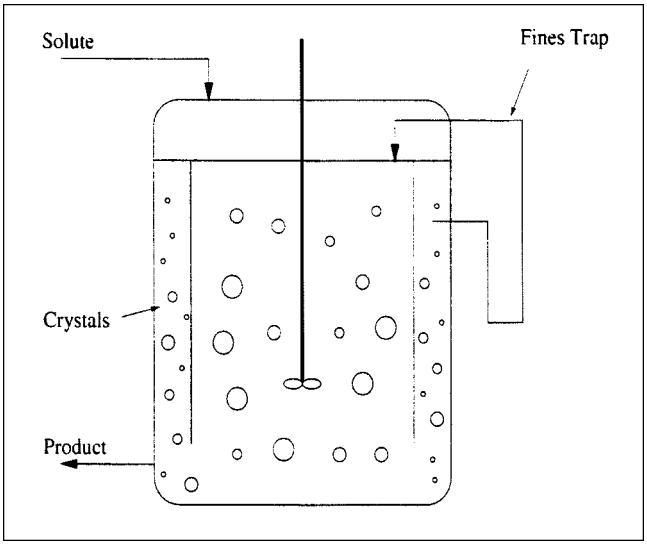

Figure 1. Continuous crystallizer with fines trap.

where $n(r,\bar{t})$ is the number of crystals of radius $r \in [0,\infty)$ at time $\bar{t}$ per unit volume of suspension; τ is the residence time; c is the solute concentration in the crystallizer; c_0 is the solute concentration in the feed; $\bar{\epsilon} = 1 - \int_0^\infty n(r,\bar{t})(4/3)\pi r^3\, dr$ is the volume of liquid per unit volume of suspension; $R(\bar{t})$ is the growth rate; $\delta(r-0)$ is the standard Dirac function; and $Q(\bar{t})$ is the nucleation rate. The rate at which crystals are circulated through the fines trap is $1/\tilde{\tau} = F_0/V$ (F_0 is the fines recirculation rate and V is the active volume of the crystallizer that is assumed to be constant) and $\bar{h}(r)$ expresses the desired selection curve for fines destruction (classification function). We assume that it is desirable to remove with the fines trap crystals of size r_m and smaller, and thus $\bar{h}(r)$ takes the form

$$\bar{h}(r) = \begin{bmatrix} 1, & \text{for } r \le r_m \\ 0, & \text{for } r > r_m \end{bmatrix}. \tag{23}$$

In the population balance, the term $\delta(r-0)Q(\bar{t})$ accounts for the production of crystals of infinitesimal (zero) size via nucleation. $R(\bar{t})$ and $Q(\bar{t})$ are assumed to follow McCabe's law and Volmer's nucleation law, respectively

$$R(\bar{t}) = k_1(c - c_s), \quad Q(\bar{t}) = \bar{\epsilon} k_2 e^{-k_3/[(c/c_s)-1]^2} \tag{24}$$

where k_1, k_2, k_3 are constants and c_s is the concentration of solute at saturation. Using the expressions for $Q(\bar{t})$ and $R(\bar{t})$, the system of Eq. 22 can be written as

$$\frac{\partial n}{\partial \bar{t}} = -k_1(c - c_s)\frac{\partial n}{\partial r} - \frac{n}{\tau} - \bar{h}(r)\frac{n}{\tilde{\tau}} + \delta(r-0)\bar{\epsilon} k_2 e^{-k_3/[(c/c_s)-1]^2}$$

$$\frac{dc}{d\bar{t}} = \frac{(c_0 - \rho)}{\bar{\epsilon}\tau} + \frac{(\rho - c)}{\tau} + \frac{(\rho - c)}{\bar{\epsilon}}\frac{d\bar{\epsilon}}{d\bar{t}}. \tag{25}$$

The multivariable control problem is formulated as the one of controlling the crystal concentration and the solute concentration, that is

$$y_1(\bar{t}) = 8\pi\sigma^3 \int_0^\infty n(r,\bar{t})\, dr = \tilde{x}_0,$$

$$y_2(\bar{t}) = \frac{[c(\bar{t}) - c_s]}{(c_0 - c_s)} = \tilde{y}(\bar{t}) \tag{26}$$

by manipulating the flow rate of suspension through the fines trap and the inlet solute concentration, that is

$$\bar{u}_1(\tilde{t}) = \frac{1}{\tilde{\tau}} - \frac{1}{\tilde{\tau}_s},$$

$$\bar{u}_2(\tilde{t}) = \frac{c_0 - c_{0_s}}{c_0 - c_s}, \tag{27}$$

where $1/\tilde{\tau}_s$ and c_{0_s} denote the circulation rate of suspension in the fines trap and the inlet concentration at steady state, respectively. Since both manipulated variables directly enter the equations that describe the dynamics of the CSD and solute concentration, the crystallizer with the crystal concentration and solute concentration as controlled outputs, and the flow rate of suspension through the fines trap and solute feed concentration as manipulated inputs is an approximately controllable system [see Semino and Ray (1995b) for a rigorous controllability analysis].

Uncertainties in the form of modeling errors in the preexponential factor of the nucleation rate, k_2, and the density of crystals, ρ, are introduced into the system. Specifically

$$k_2 = k_{2,\text{nom}} + 0.5k_{2,\text{nom}} \sin(0.5t),$$

$$\rho = \rho_{\text{nom}} + 0.1\rho_{\text{nom}}, \tag{28}$$

where $k_{2,\text{nom}}$ and ρ_{nom} represent the nominal values of the preexponential factor and the crystal density, respectively. We also consider fast and stable process dynamics arising from the dynamics of the controlled actuators and the measurement sensors. These dynamics will be completely neglected in the model used for controller design, but they will be included in the detailed process model that will be used to implement the nonlinear controller. Specifically, to account for the actuator dynamics, we consider the following dynamical system

$$\epsilon_1 \dot{z}_1 = -z_1 + z_2$$

$$\epsilon_1 \dot{z}_2 = -z_2 + \bar{u}_1$$

$$\epsilon_2 \dot{z}_3 = -z_3 + z_4$$

$$\epsilon_2 \dot{z}_4 = -z_4 + \bar{u}_2, \tag{29}$$

where z_1 and z_3 are the values that will be implemented on the process instead of $\bar{u}_1$ (flow rate of suspension through the fines trap) and $\bar{u}_2$ (inlet source concentration), and ϵ_1, ϵ_2 are positive parameters characterizing how fast the actuator dynamics are. To further explain the structure of the dynamical system of Eq. 29, note that when $\epsilon_1 = \epsilon_2 = 0$ (that is, the actuator dynamics are not explicitly modeled), then $z_1(t) = \bar{u}_1(t)$ and $z_3(t) = \bar{u}_2(t)$ for all times, and the control actions $\bar{u}_1(t)$,

$\bar{u}_2(t)$ computed by the controller are instantaneously implemented on the process. On the other hand, as ϵ_1 and ϵ_2 become greater than zero, the dynamics of the system of Eq. 29 become important and a lag in the profiles of the pairs $[z_1(t), \bar{u}_1(t)]$ and $[z_3(t), \bar{u}_2(t)]$ is created. This lag increases as ϵ_1 and ϵ_2 increase. It is the robustness of the controller with respect to this lag that we study in the simulations shown below. Similarly to the case of actuator dynamics, we assume that the sensor dynamics are described by the following dynamical system

$$\begin{aligned}
\epsilon_3 \dot{z}_5 &= -z_5 + z_6 \\
\epsilon_3 \dot{z}_6 &= -z_6 + y_1 \\
\epsilon_4 \dot{z}_7 &= -z_7 + z_8 \\
\epsilon_4 \dot{z}_8 &= -z_8 + y_2,
\end{aligned} \tag{30}$$

where z_5 and z_7 are the values of y_1 (crystal-size concentration) and y_2 (solute concentration) used in the controller, and ϵ_3, ϵ_4 are positive parameters characterizing how fast the sensor dynamics are. The models for the actuator and sensor dynamics of Eqs. 29–30 are coupled with the model of Eq. 25 leading to the full model that describes the process.

Performing a two-time-scale decomposition to the full process model, one can show that its fast dynamics are stable, and that its slow dynamics are described by the ϵ-independent model of Eq. 25, which will be used as the basis for controller synthesis. Owing to its distributed parameter nature, Eq. 25 cannot be directly used for the synthesis of model-based feedback controllers. A model-reduction procedure based on a combination of the method of moments and the approximation of the crystal-size distribution with a Laguerre series expansion is used to reduce the system of Eq. 25 into a small set of ODEs. This model-reduction procedure is motivated from the fact that the dominant dynamics of the system of Eq. 25 are characterized by a small number of degrees of freedom; the reader may refer to Chiu and Christofides (1999) for a detailed analysis of the dynamic behavior of continuous crystallizers. Defining the νth moment of $\eta(r,\bar{t})$ as

$$\mu_\nu = \int_0^\infty r^\nu n(r,\bar{t})\, dr, \qquad \nu = 0, \ldots, \tag{31}$$

multiplying the population balance in Eq. 25 by r^ν, and integrating over all crystal sizes, the following infinite set of ordinary differential equations, which describes the rate of change of all the moments of the crystal-size distribution and the solute concentration, is obtained

$$\begin{aligned}
\frac{d\mu_0}{d\bar{t}} &= -\frac{\mu_0}{\tau} - \int_0^{r_m} \frac{n(r,\bar{t})}{\tilde{\tau}}\, dr + \left(1 - \frac{4}{3}\pi\mu_3\right) k_2 e^{-k_3/[(c/c_s)-1]^2} \\
\frac{d\mu_\nu}{d\bar{t}} &= -\frac{\mu_\nu}{\tau} + \nu k_1 (c - c_s)\mu_{\nu-1} - \int_0^{r_m} r^\nu \frac{n(r,\bar{t})}{\tilde{\tau}}\, dr, \\
&\qquad\qquad \nu = 1, 2, 3, \ldots \\
\frac{dc}{d\bar{t}} &= \frac{c_0 - c - 4\pi\tau(c - c_s)\mu_2(\rho - c)}{\tau\left(1 - \frac{4}{3}\pi\mu_3\right)}.
\end{aligned} \tag{32}$$

Referring to the preceding system, note that it constitutes an unclosed set of moment equations owing to the nature of the classification function of the fines destruction. It is important to point out that when a fines trap is not used [that is, $h(r) = 0$], then the first four moment equations and the concentration equation make up a closed set of differential equations that accurately describes the dominant dynamics of the crystallizer [see Chiu and Christofides (1999) for details].

In order to close the set of moment equations, an approximate analytical expression for $n(r,\bar{t})$ in terms of the moments is needed in order to obtain a closed set of ordinary differential equations. Such an approximation using Laguerre polynomial expansion was suggested in Hulburt and Katz (1964) and takes the following form

$$n(r,\bar{t}) = \frac{\lambda}{a} p^{(\lambda)}\left(\frac{\lambda r}{a}\right) \sum_{n=0}^{\infty} \kappa_n L_n^{(\lambda)}\left(\frac{\lambda r}{a}\right), \tag{33}$$

where a and λ are functions of the moments of the crystal-size distribution that are explicit functions of time. $L_n^{(\lambda)}$ are the nth-order associated Laguerre polynomials

$$L_n^{(\lambda)}(z) = \sum_{j=0}^{\infty} (-1)^j \frac{n!(n+\lambda-1)!}{j!(n-j)!(n+\lambda-1-j)!} z^{n-j} \qquad n = 0, 1, 2, \ldots, \tag{34}$$

which are constructed by orthogonalizing the powers of z with respect to the Γ-distribution weighting function

$$p^{(\lambda)}(z) = \frac{1}{(\lambda-1)!} z^{\lambda-1} e^{-z} \tag{35}$$

and κ_n takes the following form

$$\kappa_n = \sum_{j=0}^{n} (-1)^j \frac{(\lambda-1)!}{j!(n+\lambda-1-j)!} \frac{(\lambda/a)^{n-j}}{(n-j)!} \mu_{n-j}, \tag{36}$$

with the leading terms of κ_n being

$$\begin{aligned}
\kappa_0 &= \mu_0 \\
\kappa_1 &= \frac{1}{a}\mu_1 - \mu_0 \\
\kappa_2 &= \frac{1}{2a^2}\frac{\lambda}{\lambda+1}\mu_2 - \frac{1}{a}\mu_1 + \frac{1}{2}\mu_0.
\end{aligned} \tag{37}$$

If we choose a and λ to be

$$a = \frac{\mu_1}{\mu_0} \qquad \lambda = \frac{a^2}{\mu_2/\mu_0 - a^2} \tag{38}$$

so as to force κ_1 and κ_2 to be 0, Eq. 33 becomes

$$n(r,\bar{t}) = \frac{\lambda}{a} p^{(\lambda)}\left(\frac{\lambda r}{a}\right)\left[\mu_0 + \sum_{n=3}^{\infty} \kappa_n L_n^{(\lambda)}\left(\frac{\lambda r}{a}\right)\right]. \tag{39}$$

Neglecting the terms in Eq. 39 with $n = 3$ and higher results in the following approximation for the particle-size distribution:

$$n(r,\bar{t}) = \frac{\lambda(\bar{t})}{a(\bar{t})}\, p^{(\lambda(\bar{t}))}\left(\frac{\lambda(\bar{t})r}{a(\bar{t})}\right)\mu_0. \tag{40}$$

Substituting Eq. 40 into Eq. 32 and introducing the following set of dimensionless variables and parameters:

$$t = \frac{\bar{t}}{\tau}, \quad \tilde{x}_0 = 8\pi\sigma^3\mu_0, \quad \tilde{x}_1 = 8\pi\sigma^2\mu_1, \quad \tilde{x}_2 = 4\pi\sigma\mu_2,$$

$$\tilde{x}_3 = \frac{4}{3}\pi\mu_3, \ldots, \quad \sigma = k_1\tau(c_0 - c_s), \quad Da = 8\pi\sigma^3 k_2\tau,$$

$$F = \frac{k_3 c_s^2}{(c_0 - c_s)^2}, \quad \alpha = \frac{(\rho - c_s)}{(c_0 - c_s)}, \quad \tilde{y} = \frac{(c - c_s)}{(c_0 - c_s)}, \tag{41}$$

the following system is obtained:

$$\frac{d\tilde{x}_0}{dt} = -\tilde{x}_0 + (1 - \tilde{x}_3)\, Da e^{-F/\tilde{y}^2} - 8\pi\sigma^3\mu_0\frac{\tau}{\tilde{\tau}}\frac{1}{(\lambda-1)!}\left(\frac{\lambda}{a}\right)^{\lambda}\int_0^{r_m} r^{\lambda-1}e^{-\lambda r/a}dr$$

$$\frac{d\tilde{x}_1}{dt} = -\tilde{x}_1 + \tilde{y}\tilde{x}_0 - 8\pi\sigma^2\mu_0\frac{\tau}{\tilde{\tau}}\frac{1}{(\lambda-1)!}\left(\frac{\lambda}{a}\right)^{\lambda}\int_0^{r_m} r^{\lambda}e^{-\lambda r/a}dr$$

$$\frac{d\tilde{x}_2}{dt} = -\tilde{x}_2 + \tilde{y}\tilde{x}_1 - 4\pi\sigma\mu_0\frac{\tau}{\tilde{\tau}}\frac{1}{(\lambda-1)!}\left(\frac{\lambda}{a}\right)^{\lambda}\int_0^{r_m} r^{\lambda+1}e^{-\lambda r/a}dr$$

$$\frac{d\tilde{x}_3}{dt} = -\tilde{x}_3 + \tilde{y}\tilde{x}_2 - \frac{4}{3}\pi\mu_0\frac{\tau}{\tilde{\tau}}\frac{1}{(\lambda-1)!}\left(\frac{\lambda}{a}\right)^{\lambda}\int_0^{r_m} r^{\lambda+2}e^{-\lambda r/a}dr$$

$$\vdots$$

$$\frac{d\tilde{y}}{dt} = \frac{1 - \tilde{y} - (\alpha - \tilde{y})\tilde{y}\tilde{x}_2}{1 - \tilde{x}_3}. \tag{42}$$

On the basis of the system of Eq. 42, it is clear that the moments of order four and higher do not affect those of order three and lower, which means that the dominant dynamics of the system of Eq. 32 can be adequately captured by the first four moment equations and the solute mass balance equation. The expressions of the corresponding dimensionless parameters can be obtained by substituting Eq. 28 into Eq. 41 to yield the following

$$Da = Da_{\text{nom}} + 0.5\, Da_{\text{nom}} \sin(0.5t),$$

$$\alpha = \alpha_{\text{nom}} + \frac{0.1\,\rho_{\text{nom}}}{c_0 - c_s}, \tag{43}$$

where $Da_{\text{nom}} = 8\pi\sigma^3 k_{2,\text{nom}}\tau$ and $\alpha_{\text{nom}} = [(\rho_{\text{nom}} - c_s)/(c_0 - c_s)]$. Substituting the formulation of the control problem of Eqs. 26 and 27 into the fifth-order moment model, we obtain

Table 1. Dimensionless Parameters

σ	$= k_1\tau(c_0 - c_s)$	= 1.0 mm
Da_{nom}	$= 8\pi\sigma^3 k_{2,\text{nom}}\tau$	= 200.0
F	$= k_3 c_s^2/(c_0 - c_s)^2$	= 3.0
α_{nom}	$= (\rho_{\text{nom}} - c_s)/(c_0 - c_s)$	= 40.0

a system of the following general form

$$\frac{d\tilde{x}}{dt} = \tilde{f}(\tilde{x}) + \tilde{g}_1(\tilde{x})\bar{u}_1 + \tilde{g}_2(\tilde{x})\bar{u}_2 + \tilde{w}_1(\tilde{x})\theta_1 + \tilde{w}_2(\tilde{x})\theta_2$$

$$y_1 = \tilde{h}_1(\tilde{x}) \qquad y_2 = \tilde{h}_2(\tilde{x}), \tag{44}$$

where $\tilde{x}$ denotes the vector $[\tilde{x}_0\ \tilde{x}_1\ \tilde{x}_2\ \tilde{x}_3\ \tilde{y}]^T$, $\tilde{f}(\tilde{x})$, $\tilde{g}_1(\tilde{x})$ and $\tilde{g}_2(\tilde{x})$ are vector functions; and $\tilde{h}_1(\tilde{x})$ and $\tilde{h}_2(\tilde{x})$ are scalar functions whose explicit form is omitted for brevity.

Utilizing the formula of Theorem 1, we synthesize a robust nonlinear controller on the basis of the model of Eq. 44, which has the following form

$$\bar{u}_1(t) = \left[\beta_{12} L_{\tilde{g}_1}\tilde{h}(\omega)\right]^{-1}\left\{\upsilon_1 - \beta_{10}y_1 - \beta_{11}L_{\tilde{f}}\tilde{h}_1(\omega) - \chi_1\frac{y_1 - \upsilon_1}{|y_1 - \upsilon_1| + \phi_1}0.5\, Da_{\text{nom}}|(1 - \omega_3)e^{-F/\omega_4^2}|\right\}$$

$$\bar{u}_2(t) = \left[\beta_{22} L_{\tilde{g}_2}\tilde{h}(\omega)\right]^{-1}\left\{\upsilon_2 - \beta_{20}y_1 - \beta_{21}L_{\tilde{f}}\tilde{h}_2(\omega) - \chi_2\frac{y_2 - \upsilon_2}{|y_2 - \upsilon_2| + \phi_2}\frac{0.1\,\rho_{\text{nom}}}{(c_0 - c_s)}\left|\frac{\omega_4\omega_2}{1 - \omega_3}\right|\right\}, \tag{45}$$

where υ_1 and υ_2 are the set points for the two outputs, and β_{10}, β_{11}, β_{12}, β_{20}, β_{21}, β_{22}, Da_{nom}, ρ_{nom}, ϕ_1, ϕ_2, χ_1, χ_2 are parameters that are given in Tables 1, 2, and 3. The practical implementation of the robust nonlinear controller of Eq. 45 is achieved by employing the following nonlinear state ob-

Table 2. Controller Parameters

$\beta_{10} = 1$	$L_1 = [1\ 0\ 0\ 0\ 0]^T$
$\beta_{11} = 1.5$	$L_2 = [0\ 0\ 0\ 0\ 1]^T$
$\beta_{12} = 1.5$	$\phi_1 = 0.0022$
$\beta_{20} = 1$	$\phi_2 = 0.009$
$\beta_{21} = 1.5$	$\chi_1 = 1.53$
$\beta_{22} = 1.5$	$\chi_2 = 5.48$

Table 3. Process Parameters

c_0	= 1,000.0 kg·m^{-3}
c_s	= 980.2 kg·m^{-3}
ρ_{nom}	= 1,770.0 kg·m^{-3}
τ	= 1.0 h
$1/\tilde{\tau}_s$	= 0.0 h^{-1}
k_1	= 5.065×10^{-2} mm·m^3·kg^{-1}·h^{-1}
$k_{2,\text{nom}}$	= 7.958 mm^{-3}·h^{-1}
k_3	= 1.217×10^{-3}
r_m	= 1 mm

server

$$\frac{d\omega_0}{dt} = -\omega_0 + (1-\omega_3)\,Da e^{-F/\tilde{y}^2} - \bar{u}_1(t) 8\pi\sigma^3\mu_0\tau \frac{1}{(\lambda-1)!}\left(\frac{\lambda}{a}\right)^{\lambda}\int_0^{r_m} r^{\lambda-1}e^{-\lambda r/a}dr + L_{10}\left[\tilde{h}_1(\tilde{x})-\tilde{h}_1(\omega)\right] + L_{20}\left[\tilde{h}_2(\tilde{x})-\tilde{h}_2(\omega)\right]$$

$$\frac{d\omega_1}{dt} = -\omega_1 + \tilde{y}\omega_0 - \tilde{u}_1(t) 8\pi\sigma^2\mu_0\tau \frac{1}{(\lambda-1)!}\left(\frac{\lambda}{a}\right)^{\lambda} \times \int_0^{r_m} r^{\lambda}e^{-\lambda r/a}dr + L_{11}\left[\tilde{h}_1(\tilde{x})-\tilde{h}_1(\omega)\right] + L_{21}\left[\tilde{h}_2(\tilde{x})-\tilde{h}_2(\omega)\right]$$

$$\frac{d\omega_2}{dt} = -\omega_2 + \tilde{y}\omega_1 - \bar{u}_1(t) 4\pi\sigma\mu_0\tau \frac{1}{(\lambda-1)!}\left(\frac{\lambda}{a}\right)^{\lambda} \times \int_0^{r_m} r^{\lambda+1}e^{-\lambda r/a}dr + L_{12}\left[\tilde{h}_1(\tilde{x})-\tilde{h}_1(\omega)\right] + L_{22}\left[\tilde{h}_2(\tilde{x})-\tilde{h}_2(\omega)\right]$$

$$\frac{d\omega_3}{dt} = -\omega_3 + \tilde{y}\omega_2 - \bar{u}_1(t)\frac{4}{3}\pi\mu_0\tau \frac{1}{(\lambda-1)!}\left(\frac{\lambda}{a}\right)^{\lambda} \times \int_0^{r_m} r^{\lambda+2}e^{-\lambda r/a}dr + L_{13}\left[\tilde{h}_1(\tilde{x})-\tilde{h}_1(\omega)\right] + L_{23}\left[\tilde{h}_2(\tilde{x})-\tilde{h}_2(\omega)\right]$$

$$\frac{d\omega_4}{dt} = \frac{1-\omega_4-(\alpha-\omega_4)\omega_4\omega_2}{1-\omega_3} + \frac{1}{1-\tilde{\omega}_3}\bar{u}_2(t) + L_{14}\left[\tilde{h}_1(\tilde{x})-\tilde{h}_1(\omega)\right] + L_{24}\left[\tilde{h}_2(\tilde{x})-\tilde{h}_2(\omega)\right], \quad (46)$$

where ω denotes the observer state vector whose dimension is equal to that of $\tilde{x}$, and $\tilde{h}_1(\tilde{x})$, and $\tilde{h}_2(\tilde{x})$ are the measured outputs. The state observer of Eq. 46 consists of a replica of the system of Eq. 44 plus two linear gain vectors $L_1 = [L_{10}\ L_{11}\ L_{12}\ L_{13}\ L_{14}]$ and $L_2 = [L_{20}\ L_{21}\ L_{22}\ L_{23}\ L_{24}]$ multiplying the discrepancy between the actual and the estimated values of the outputs. The values of the gains L_1 and L_2 are given in Table 2. The practical implementation of the nonlinear robust output feedback controller of Eqs. 45–46 requires online measurements of the controlled outputs, $\tilde{x}_0$ (crystal concentration), and $\tilde{y}$ (solute concentration); in practice, measurements of $\tilde{x}_0$ can be obtained by using, for example, light scattering [see Bohren and Huffman (1983) and Rawlings et al. (1993) for details], and measurements of $\tilde{y}$ can be obtained by using a mass spectrometer.

The performance of the nonlinear robust output feedback controller of Eqs. 45–46 was tested through numerical simulations. The values of the system parameters and the ones in their corresponding dimensionless forms (Eq. 41) are shown in Tables 3 and 1, respectively. In all simulation runs, the following initial condition

$$n(r,0) = (2.189\times10^3)e^{-1.168r}\ \text{mm}^{-4}, \qquad c(0) = 992.1\ \text{kg}\cdot\text{m}^{-3} \quad (47)$$

was used for the process model of Eq. 25 and the finite difference method with 1000 discretization points was used for the simulations. The initial conditions for the observer states were computed numerically by using the initial conditions of Eq. 47. We note that even though the number of discretization points, 1,000, used to solve the system of Eq. 22 is very large (owing to the poor convergence properties of the finite difference scheme), the computation of an accurate (that is, independent of the discretization) solution is critical for the thorough evaluation of the performance of a nonlinear feedback controller synthesized on the basis of a low-order approximation of the distributed parameter system of Eq. 22. The adequacy of 1,000 discretization points to yield an accurate solution was established through extensive simulations of the open- and closed-loop systems.

In the first set of simulation runs, we implemented the nonlinear robust multivariable controller on the crystallizer model of Eq. 25 with the actuator dynamics of Eq. 29 in the presence of parametric uncertainty in the preexponential factor of the nucleation rate, k_2, and the density of crystals, ρ. A 0.03 decrease in the value of the set point from the initial

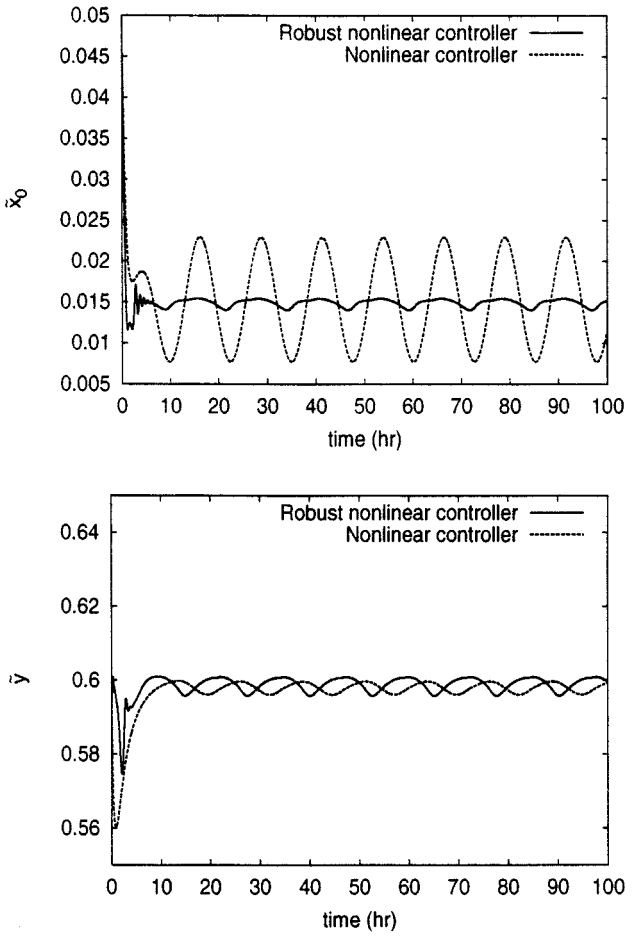

Figure 2. Closed-loop output profiles for $\tilde{x}_0$ (top plot) and $\tilde{y}$ (bottom plot) under robust nonlinear controller (solid line) and nonlinear controller that does not account for uncertainty (dashed line).

Actuator dynamics are included in the process model.

conditions was applied to the first controlled output, $\tilde{x}_0$ ($\upsilon_1 = 0.015$), while the set point for the second output, $\tilde{y}$, was set to be the same as the initial conditions ($\upsilon_2 = 0.5996$). The closed-loop output profiles are shown in Figure 2 (solid lines) with $\epsilon_1 = 0.1$ for the first manipulated input (flow rate of suspension through fines trap) and $\epsilon_2 = 0.02$ for the second manipulated input (inlet solute concentration); these are the largest values for ϵ_1, ϵ_2 for which an acceptable closed-loop output response is achieved with stability. Clearly the controller regulates the outputs to the set point values attenuating the effect of the time-varying uncertainty on the process outputs and being robust to unmodeled actuator dynamics. Figure 3 shows the profiles of the manipulated inputs (solid lines). It is observed that the control action computed by the robust controller exhibits an oscillatory behavior in order to compensate for the time variation of the parameter *Da*. For the sake of comparison, we also implemented the nonlinear multivariable controller of Eq. 45 with $\chi = 0$ (that is, no uncertainty compensation is included in the controller). Figure 2 displays the closed-loop output profiles (dashed lines), and Figure 3 displays the corresponding manipulated input profiles (dashed lines). Clearly, this controller cannot compensate for the effect of the time-varying uncertainty leading to very poor closed-loop performance. Finally, to evaluate the ability of the controller in attenuating the effect of the time-varying uncertain variables in the entire CSD, the closed-loop profile of the evolution of the CSD under robust nonlinear control is shown in Figure 4 (bottom plot) and compared to that of the open-loop process (top plot). It is obvious that fluctuations in the CSD are effectively damped by the use of robust nonlinear control.

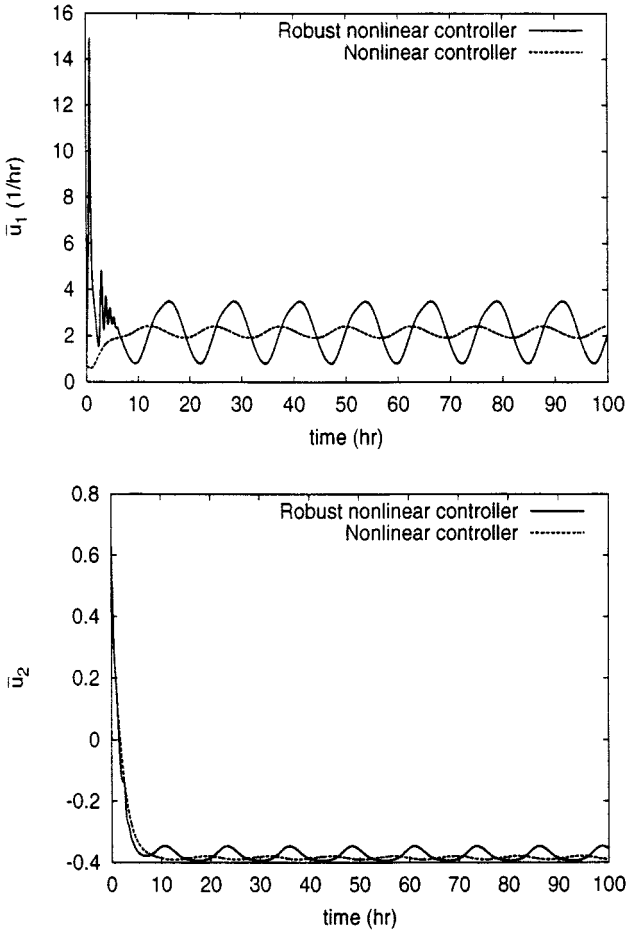

Figure 3. Manipulated input profiles for $\bar{u}_1$ (top plot) and $\bar{u}_2$ (bottom plot) under robust nonlinear controller (solid line) and nonlinear controller that does not account for uncertainty (dashed line).

Actuator dynamics are included in the process model.

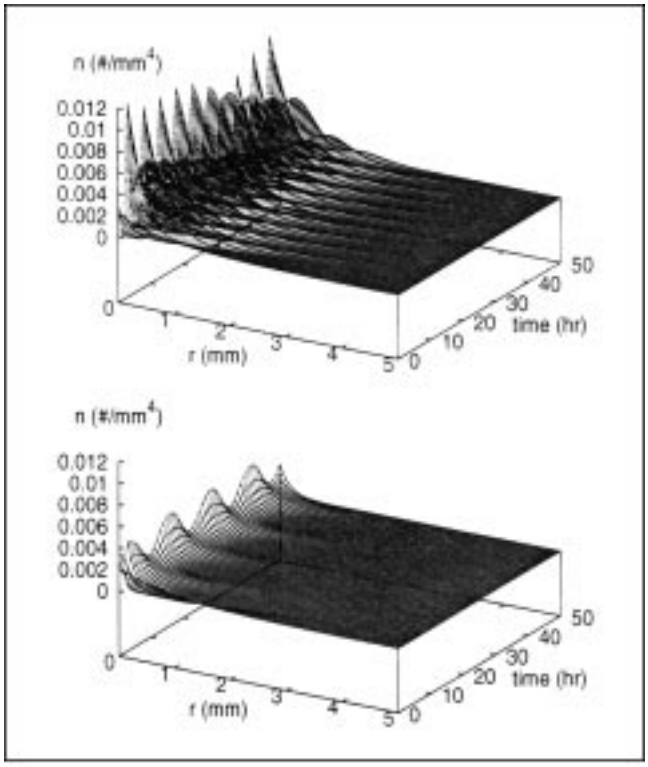

Figure 4. Profile of evolution of crystal-size distribution, open-loop (top plot), and closed loop under robust nonlinear controller (bottom plot).

Actuator dynamics are included in the process model.

In the second set of simulation runs, we implemented the nonlinear robust multivariable controller on the crystallizer model of Eq. 25 with the actuator dynamics of Eq. 29 and the sensor dynamics of Eq. 30 in the presence of the same parametric uncertainty considered in the first set of simulation runs. Again, a 0.03 decrease in the value of the set point from the initial conditions was applied to the first controlled output, $\tilde{x}_0$ ($\upsilon_1 = 0.015$), while the set point for the second controlled output, $\tilde{y}$, was set to be $\upsilon_2 = 0.5996$. The closed-loop output profiles are shown in Figure 5 (solid lines), with $\epsilon_1 = 0.1$ for the first manipulated input (flow rate of suspension through fines trap), $\epsilon_2 = 0.02$ for the second manipulated input (inlet solute concentration), $\epsilon_3 = 0.01$ for the first measured output (crystal concentration), $\epsilon_4 = 0.01$ for the second measured output (solute concentration); these are the largest values for ϵ_1, ϵ_2, ϵ_3, ϵ_4 for which an acceptable closed-loop output response is achieved with stability. Clearly, the controller regulates the outputs to the set point values minimizing the effect of the time-varying uncertainty. We also

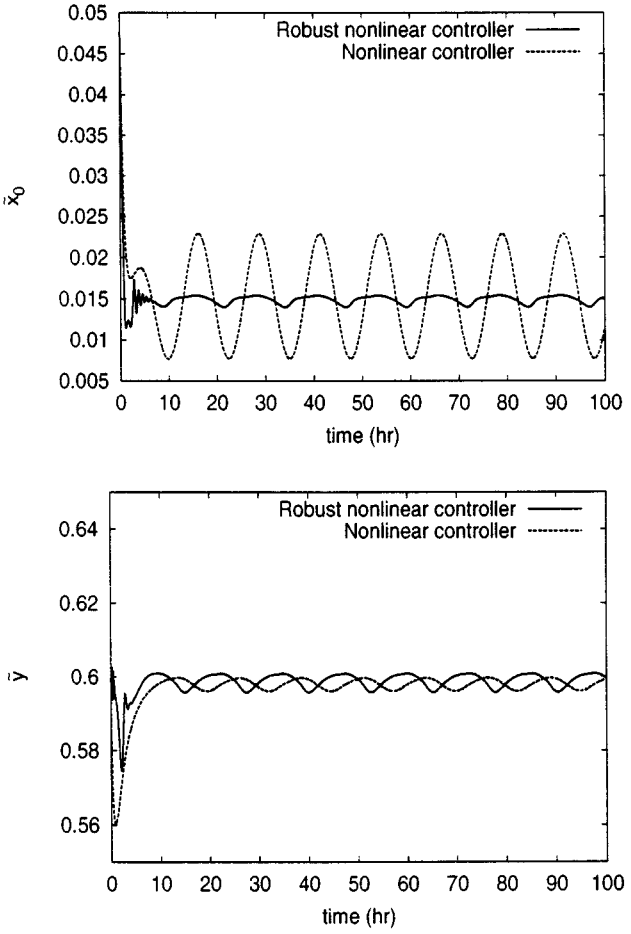

Figure 5. Closed-loop output profiles for $\tilde{x}_0$ (top plot) and $\tilde{y}$ (bottom plot) under robust nonlinear controller (solid line) and nonlinear controller that does not account for uncertainty (dashed line).

Actuator and sensor dynamics are included in the process model.

implemented the nonlinear multivariable controller of Eq. 45 with $\chi = 0$ (that is, no uncertainty compensation is included in the controller). Figure 5 shows the closed-loop output profiles (dashed lines). It is clear that this controller cannot attenuate the effect of the uncertainty on the outputs leading to poor performance. Figure 6 shows the profiles of the manipulated inputs of the robust controller (solid lines) and the ones of the nonlinear controller that does not compensate for uncertainty (dashed lines). Again, the control actions computed by the robust controller exhibit oscillatory behavior to compensate for the time-varying uncertainty. Finally, the ability of the robust nonlinear controller to attentuate the uncertainty also can be seen in Figure 7 (bottom plot) where the evolution of the CSD under robust nonlinear control is shown and compared with the open-loop profile (top plot).

Remark 11. It is important to note that we have also performed simulations of the process under proportional-integral control and obtained a very poor closed-loop performance (worse than the performance obtained under nonlinear control without uncertainty compensation). This is expected because proportional-integral control cannot effectively deal with the presence of time-varying uncertainty and significant nonlinearities in the process model. These simulations are not included in the article for reasons of brevity.

Conclusions

We developed a general method for the synthesis of practically implementable robust nonlinear controllers for a broad class of particulate processes described by population balances that explicitly handle time-varying uncertain variables (such as unknown process parameters and disturbances) and unmodeled dynamics (such as fast actuator and sensor dynamics not included in the process model used for controller design). The robust controllers are synthesized on the basis of the uncertain population balances via Lyapunov's direct method and enforce stability in the closed-loop system, attenuation of the effect of uncertain variables, and achieve particle-size distributions with desired characteristics. The robustness of the proposed controllers with respect to stable and

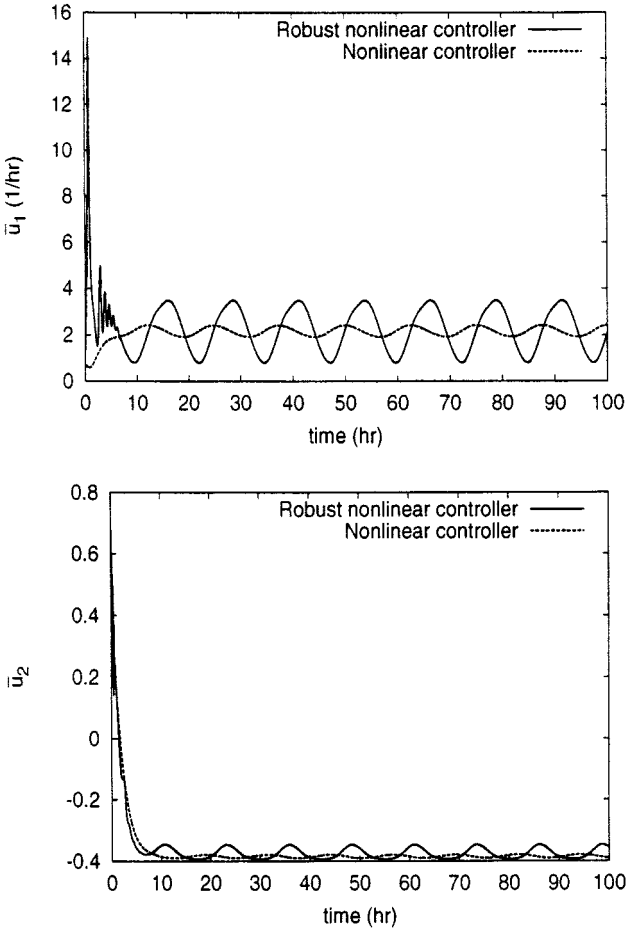

Figure 6. Manipulated input profiles for $\bar{u}_1$ (top plot) and $\bar{u}_2$ (bottom plot) under robust nonlinear controller (solid line) and nonlinear controller that does not account for uncertainty (dashed line).

Actuator and sensor dynamics are included in the process model.

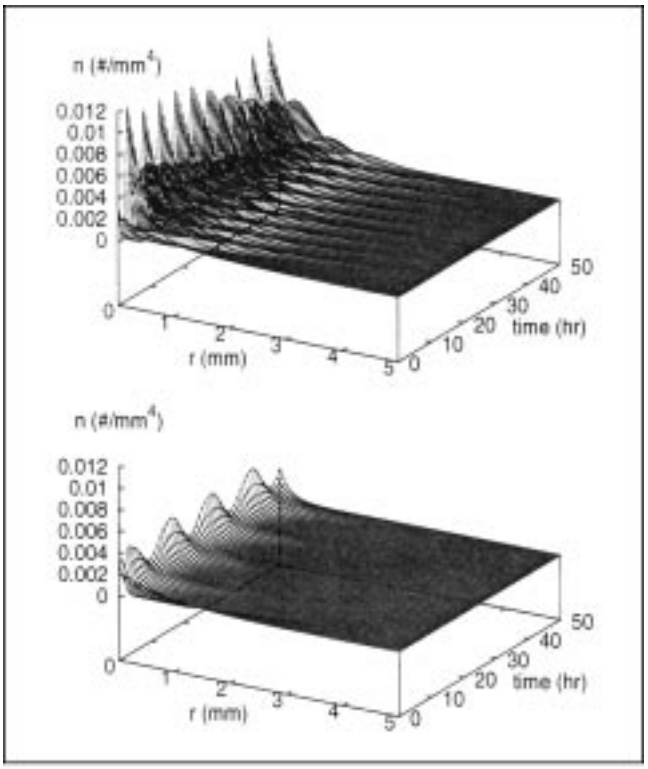

Figure 7. Profile of evolution of crystal-size distribution, open-loop (top plot), and closed loop under robust nonlinear controller (bottom plot).

Actuator and sensor dynamics are included in the process model.

sufficiently fast unmodeled dynamics was established through a singular perturbation analysis. The controllers were applied to a continuous crystallizer with fines trap in which the nucleation rate and the crystal density change with time and the actuator and sensor dynamics are not included in the model used for the synthesis of the controller. Simulation runs of the closed-loop system clearly demonstrated the ability of the controllers to attenuate the uncertainty and achieve a crystal-size distribution with desired characteristics, and documented their superiority over nonlinear controllers that do not account for the presence of uncertainty.

Acknowledgment

Financial support from a National Science Foundation CAREER award, CTS 9733509, is gratefully acknowledged.

Literature Cited

Balas, M. J., ''Finite-Dimensional Direct Adaptive Control for Discrete-Time Infinite-Dimensional Linear Systems,'' *J. Math. Anal. Appl.*, **196**, 153 (1995).

Bohren, C. F., and D. R. Huffman, *Absorption and Scattering of Light by Small Particles*, Wiley, New York (1983).

Byrnes, C. I., ''Adaptive Stabilization of Infinite Dimensional Linear Systems,'' *26th IEEE Conf. on Decision and Control*, Los Angeles, CA, p. 1435 (1987).

Chiu, T., and P. D. Christofides, ''Nonlinear Control of Particulate Processes,'' *AIChE J.*, **45**, 1279 (1999).

Christofides, P. D., ''Robust Control of Parabolic PDE Systems,'' *Chem. Eng. Sci.*, **53**, 2949 (1998).

Christofides, P. D., *Nonlinear and Robust Control of PDE Systems: Methods and Applications to Transport-Reaction Processes*, Birkhäuser, Boston (2000).

Christofides, P. D., ''Robust Output Feedback Control of Nonlinear Singularly Perturbed Systems,'' *Automatica*, **36**, 45 (2000).

Christofides, P. D., and P. Daoutidis, ''Robust Control of Hyperbolic PDE Systems,'' *Chem. Eng. Sci.*, **53**, 85 (1998).

Daoutides, P., and P. D. Christofides, ''Dynamic Feedforward/Output Feedback Control of Nonlinear Processes,'' *Chem. Eng. Sci.*, **50**, 1889 (1995).

Demetriou, M. A., ''Model Reference Adaptive Control of Slowly Time-Varying Parabolic Systems,'' *Proc. 33rd IEEE Conf. on Decision and Control*, Orlando, FL, p. 775 (1994).

Dimitratos, J., G. Elicabe, and C. Georgakis, ''Control of Emulsion Polymerization Reactors,'' *AIChE J.*, **40**, 1993 (1994).

Eaton, J. W., and J. B. Rawlings, ''Feedback Control of Chemical Processes Using On-line Optimization Techniques,'' *Comput. Chem. Eng.*, **14**, 469 (1990).

Hill, P. J., and K. M. Ng, ''New Discretization Procedure for the Agglomeration Equation,'' *AIChE J.*, **42**, 727 (1996).

Holmes, P., J. L. Lumley, and G. Berkooz, *Turbulence, Coherent Structures, Dynamical Systems and Symmetry*, Cambridge Univ. Press, New York (1996).

Hounslow, M. J., ''A Discretized Population Balance for Continuous Systems at Steady-State,'' *AIChE J.*, **36**, 106 (1990).

Hulburt, H. M., and S. Katz, ''Some Problems in Particle Technology: A Statistical Mechanical Formulation,'' *Chem. Eng. Sci.*, **19**, 555 (1964).

Isidori, A., *Nonlinear Control Systems: An Introduction*, 2nd ed., Springer-Verlag, Berlin-Heidelberg (1989).

Jerauld, G. R., Y. Vasatis, and M. F. Doherty, ''Simple Conditions for the Appearance of Sustained Oscillations in Continuous Crystallizers,'' *Chem. Eng. Sci.*, **38**, 1675 (1983).

Kokotovic, P. V., H. K. Khalil, and J. O'Reilly, *Singular Perturbations in Control: Analysis and Design*, Academic Press, London (1986).

Kumar, A., P. D. Christofides, and P. Daoutidis, ''Singular Perturbation Modeling and Control of Nonlinear Two-Time-Scale Processes with Non-Explicit Time-Scale Multiplicity,'' *Chem. Eng. Sci.*, **53**, 1491 (1998).

Kumar, S., and D. Ramkrishna, ''On the Solution of Population Balance Equations by Discretization—I. A Fixed Pivot Technique,'' *Chem. Eng. Sci.*, **51**, 1311 (1996a).

Kumar, S., and D. Ramkrishna, ''On the Solution of Population Balance Equations by Discretization—II. A Moving Pivot Technique,'' *Chem. Eng. Sci.*, **51**, 1333 (1996b).

Kurtz, M. J., and G.-Y. Zhu, A. Zamamiri, M. A. Henson, and M. A. Hjortso, ''Control of Oscillating Microbial Cultures Described by Population Balance Models,'' *Ind. Eng. Chem. Res.*, **37**, 4059 (1998).

Landgrebe, J. D., and S. E. Pratsinis, ''A Discrete Sectional Model for Particulate Production by Gas Phase Chemical Reaction and Aerosol Coagulation in the Free Molecular Regime,'' *J. Colloid Interface Sci.*, **139**, 63 (1990).

Lei, S. J., R. Shinnar, and S. Katz, ''The Stability and Dynamic Behavior of a Continuous Crystallizer with a Fines Trap,'' *AIChE J.*, **17**, 1459 (1971).

Ramkrishna, D., ''The Status of Population Balances,'' *Rev. Chem. Eng.*, **3**, 49 (1985).

Randolph, A. D., and M. A. Larson, *Theory of Particulate Processes*, 2nd ed., Academic Press, San Diego (1988).

Rawlings, J. B., S. M. Miller, and W. R. Witkowski, ''Model Identification and Control of Solution Crystallization Processes,'' *Ind. Eng. Chem. Res.*, **32**, 1275 (1993).

Rawlings, J. B., and W. H. Ray, ''Emulsion Polymerization Reactor Stability: Simplified Model Analysis,'' *AIChE J.*, **33**, 1663 (1987a).

Rawlings, J. B., and W. H. Ray, ''Stability of Continuous Emulsion Polymerization Reactors: A Detailed Model Analysis,'' *Chem. Eng. Sci.*, **42**, 2767 (1987b).

Rohani, S., and J. R. Bourne, ''Self-Tuning Control of Crystal Size Distribution in a Cooling Batch Crystallizer,'' *Chem. Eng. Sci.*, **12**, 3457 (1990).

Semino, D., and W. H. Ray, ''Control of Systems Described by Population Balance Equations—I. Controllability Analysis,'' *Chem. Eng. Sci.*, **50**, 1805 (1995a).

Semino, D., and W. H. Ray, ''Control of Systems Described by Popu-

lation Balance Equations—II. Emulsion Polymerization with Constrained Control Action,'' *Chem. Eng. Sci.*, **50**, 1825 (1995b).
Wen, J. T., and M. J. Balas, ''Robust Adaptive Control in Hilbert Space,'' *J. Math. Anal. Appl.*, **143**, 1 (1989).
Ydstie, E. B., and A. A. Alonso, ''Process Systems and Passivity via the Clausius-Planck Inequality,'' *Syst. Contr. Lett.*, **30**, 253 (1997).
Ydstie, E. B., and P. V. Krishnan, ''From Thermodynamics to a Macroscopic Theory for Process Control,'' AIChE Meeting, San Francisco, CA (1994).

Appendix: Proof of Theorem 1

Substituting the controller of Eq. 19 into the particulate process model of Eq. 1, we obtain:

$$\frac{\partial n}{\partial t} = -\frac{\partial\left[G(x,r)n\right]}{\partial r} + \bar{w}\left[n, x, r, z, \theta(t)\right] + \bar{g}_1(n, x, r)\, a(\tilde{x}, \bar{v}, t), \qquad n(0,t) = b\left[x(t)\right]$$

$$\dot{x} = \bar{f}(x) + Q_1(x)z + \bar{g}_2(x)\, a(\tilde{x}, \bar{v}, t) + \bar{g}_3\left[x, \theta(t), \int_0^{r_{\max}} a_2(n, r, x)\, dr\right]$$

$$\epsilon \dot{z} = \tilde{f}(x) + Q_2(x)z + \tilde{g}_2(x)\, a(\tilde{x}, \bar{v}, t) + \tilde{g}_3\left[x, \theta(t), \int_0^{r_{\max}} a_2(n, r, x)\, dr\right]. \quad (48)$$

Performing a decomposition of the preceding system into the fast and slow time-scales, we obtain the following system that describes the fast dynamics of the closed-loop system:

$$\frac{dz}{d\tau} = \bar{f}(x) + Q_2(x)z + \tilde{g}_2(x)\, a(\tilde{x}, \bar{v}, t) + g_3\left[x, \theta(t), \int_0^{r_{\max}} a_2(n, r, x)\, dr\right]. \quad (49)$$

Since the feedback law $a(\tilde{x}, \bar{v}, t)$ does not use feedback of the fast state z, the preceding system is exponentially stable. Setting $\epsilon = 0$, the system that describes the slow dynamics of the closed-loop system is obtained:

$$\frac{\partial n}{\partial t} = -\frac{\partial\left[G(x,r)n\right]}{\partial r} + w\left[n, x, r, \theta(t)\right] + g_1(n, x, r)\, a(\tilde{x}, \bar{v}, t), \qquad n(0,t) = b\left[x(t)\right]$$

$$\dot{x} = f(x) + g_2(x)\, a(\tilde{x}, \bar{v}, t) + g_3\left[x, \theta(t), \int_0^{r_{\max}} a_2(n, r, x)\, dr\right]. \quad (50)$$

Applying the method of weighted residuals to the above system, we obtain:

$$\int_0^{r_{\max}} \psi_\nu(r) \sum_{k=1}^{N} \phi_k(r) \frac{\partial a_{kN}(t)}{\partial t}\, dr = -\sum_{k=1}^{N} a_{kN}(t) \int_0^{r_{\max}} \psi_\nu(r) \frac{\partial\left[G(x_N, r)\phi_k(r)\right]}{\partial r}\, dr + \int_0^{r_{\max}} \psi_\nu(r)\, w\left[\sum_{k=1}^{N} a_{kN}(t)\phi_k(r), x_N, r, \theta(t)\right] dr + \int_0^{r_{\max}} \psi_\nu(r)\, g_1\left[\sum_{k=1}^{N} a_{kN}(t)\phi_k(r), x_N, r\right] a(\tilde{x}, \bar{v}, t)\, dr, \qquad \nu = 1, \ldots, N$$

$$\dot{x}_N = f(x_N) + g_2(x_N)\, a(\tilde{x}, \bar{v}, t) + g_3\left\{x_N, \theta(t), \int_0^{r_{\max}} a_2\left[\sum_{k=1}^{N} a_{kN}(t)\phi_k(r), r, x_N\right] dr\right\}$$

$$y_{si}(t) = h_i\left[\int_0^{r_{\max}} c_\kappa \sum_{k=1}^{N} a_{kN}(t)\phi_k(r)\, dr, x_N\right], \qquad i = 1, \ldots, m, \quad \kappa = 1, \ldots, l, \quad (51)$$

or using the vector notation,

$$\dot{\tilde{x}} = \tilde{f}(\tilde{x}) + \sum_{i=1}^{m} \tilde{g}_i(\tilde{x})\, a_i(\tilde{x}, \bar{v}, t) + \tilde{w}(\tilde{x}, \theta)$$

$$y_{s_i} = \tilde{h}_i(\tilde{x}), \qquad i = 1, \ldots, m. \quad (52)$$

For the preceding system we showed in Christofides (1998) that if assumptions 1, 2, and 3 hold, then there exists a positive real number δ, such that if $\max\{|\tilde{x}(0)|, \|\theta\|, \|\dot{\theta}\|, \|\tilde{v}\|\} \le \delta$, then its state is bounded and its outputs satisfy $\limsup_{t\to\infty} |y_{s_i}(t) - v_i| \le O(\phi)$, $i = 1, \ldots, l$. Finally, since the fast subsystem of Eq. 49 is exponentially stable, we can use standard singular perturbation arguments to show that there exist positive real numbers (δ, ϕ^*, d) such that for each $\phi \le \phi^*$, there exists $\epsilon^*(\phi)$, such that if $\phi \le \phi^*$, $\epsilon \le \epsilon^*(\phi)$ and $\max\{|x(0)|, |z(0)|, \|n(r,0)\|_2, \|\theta\|, \|\dot{\theta}\|, \|\tilde{v}\|\} \le \delta$, then the state of the closed-loop system is bounded and that is outputs satisfy the relation of Eq. 20.

Manuscript received June 28, 1999, and revision received Oct. 1, 1999.